京都大学　理学研究科・理学部
GRADUATE SCHOOL OF FACULTY OF SCIENCE KYOTO UNIVERSITY

JST MIRAI 未来社会創造事業

Topological Flow Data Analysis (TFDA) Theory and Applications to Atmospheric and Ocean Flows

TAKASHI SAKAJO (Kyoto University)

Collaborators:
Mathematics: Tomoo Yokoyama (Saitama) , Tomoki Uda (Toyama) ,
Shizuo Kaji (Kyushu), Kazuki Koga (Tokyo Inst. Tech.)
Meteorology: Masaru Inatsu (Hokkaido)
Oceanology: Shun Oishi (RIKEN)
Medicine: Kei-ichi Itatani (Nagoya City University),

2024 Sept. 23, Univ. Rouen France

Motivation – complex flow patterns

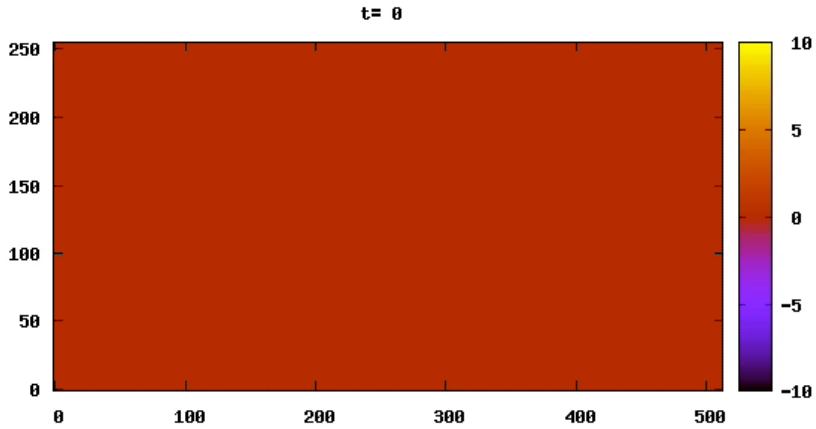

A flow around a wing (Sawamura 2012)

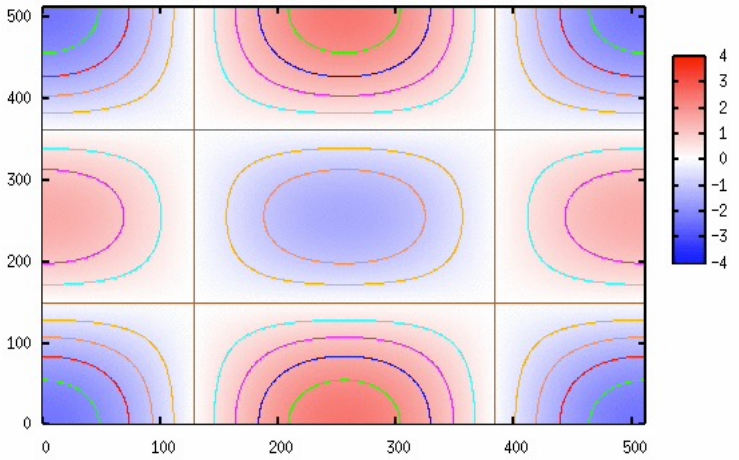

2D Couette flow (S. 2006)

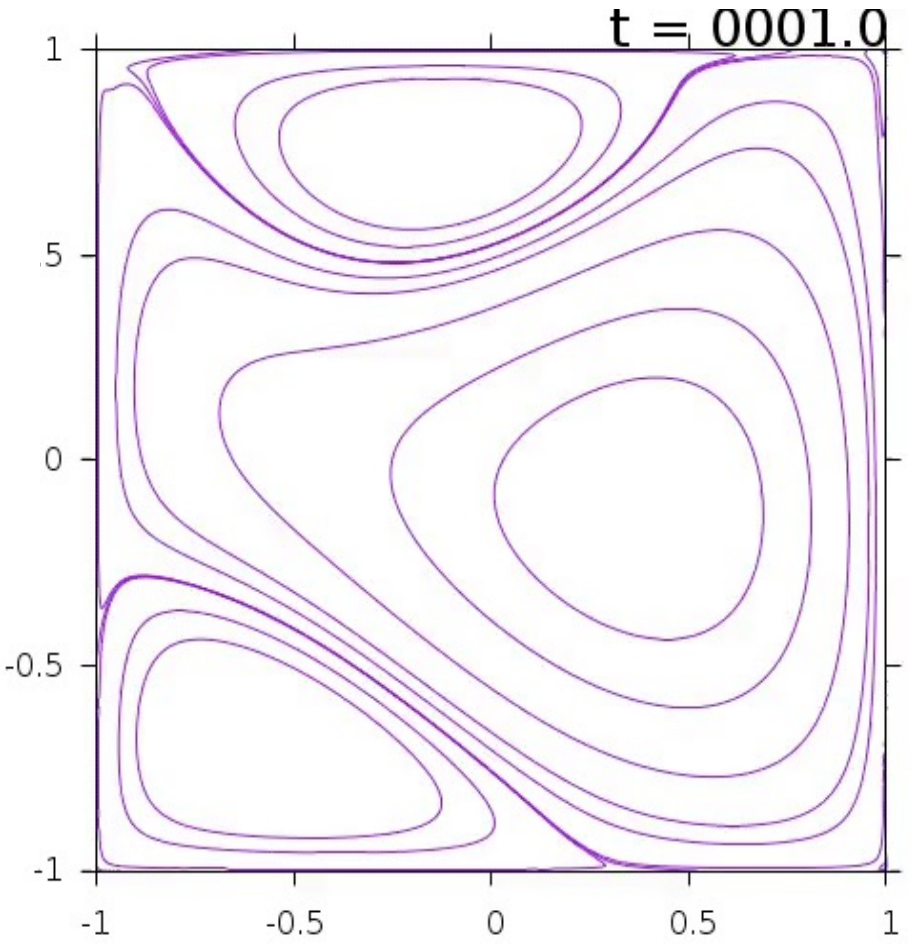

A flow model of rotating flow in a box.
(Matsumoto 2015)

We develop flow pattern characterizations to promote interdisciplinary research using flow simulations and experiments.

What is Topological Flow Data Analysis (TFDA)?

- It is a method of data analysis extracting topological features of flow orbits generated by 2D vector fields.

- **(A reduced-order modeling with discrete graphs)**
  The continuous time evolution of flows is reduced to a discrete dynamical system of graphs (partially Cyclically Ordered rooted Tree = COT) and its symbolic representation (COT representation).

- **(Quantitative estimation of flow topology)**
  It extracts quantitative information associated with topological flow patterns in datasets.

- We explain the basic features of TFDA using 2D incompressible flows, and we then extend the theory suitable for blood flows in the heart.

Reference: Incompressible flows: Proc. Roy. Soc. A '13, Physica D '15, IMA J. Appl. Math. '18; Compressible flows: Disc. Math. Algo. Appl. '22

Topological classification of flow orbits

Poincaré-Hopf Theorem + Poincaré-Bendixson Theorem

Let v be a vector field on a compact smooth manifold M with isolated N singular points and solid boundary satisfying slip boundary condition. Then it satifies

$$\sum_{i=1}^{N} \mathrm{ind}_{x_i}(v) = \chi(M),$$

where $\chi(M)$ is the Euler characteristic of M, $\mathrm{ind}_{x_i}(v)$ denotes the index of v at the singular orbit $x_i \in M$ for $i = 1, \cdots, N$.

Index of singular points in vector fields

A center: index = **+1**

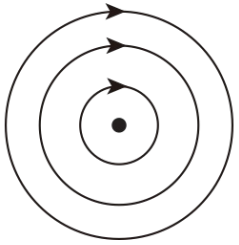

A saddle: index= **-1**

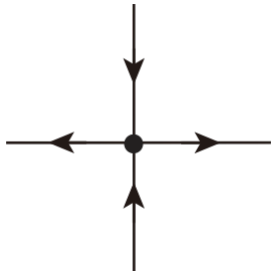

A saddle at boundary: index **-1/2**

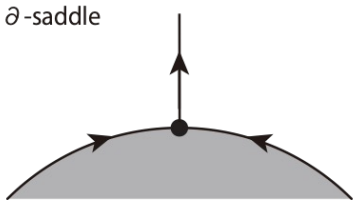

A dipole singularity: index= **2**

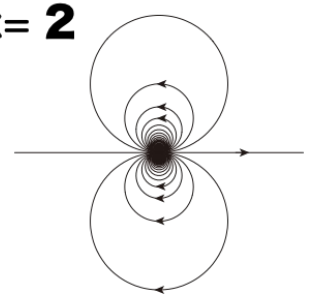

Euler characteristic of a spherical surface

$$\chi(M) = 2 - b \qquad b \text{ the number of boundaries}$$

TFDA for 2D structurally Hamiltonian vector field

Hamiltonian (incompressible) vector fields with the slip boundary condition

$\psi(t,x,y)$: stream function

$\boldsymbol{u}(t,\boldsymbol{x}) = (u(t,x,y), v(t,x,y))$

$$u = \frac{\partial \psi}{\partial y} \qquad v = -\frac{\partial \psi}{\partial x}$$

We consider the topological structure of **orbits** generated by the instantaneous Hamiltonian vector fields.

$$\nabla\psi \cdot \boldsymbol{u} = 0$$

Streamlines = Level curves of the stream function

Structurally stable Hamiltonian vector fields.

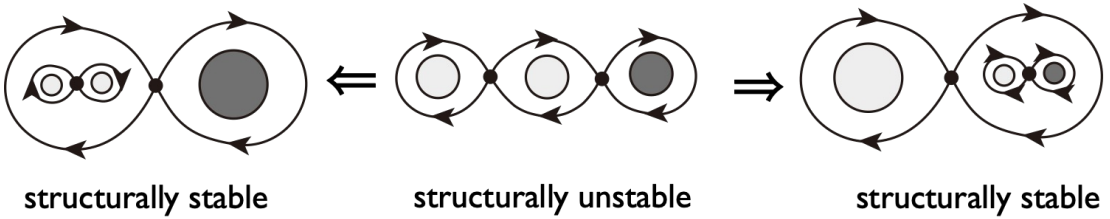

Topological structure theorem for Hamiltonian flows in the uniform flow

Theorem 2 *The Hamiltonian vector field $V \in \chi_1^r$ is structurally stable, if and only if*

(1) *the restriction of V on the complement of the 1-source-sink point is regular,*

(2) *all saddle connections are homoclinic connections,*

(3) *all ∂-saddle connections connect two ∂-saddles located at the same boundary.*

Theoretical Overview of TFDA for 2D incompressible flows

COT symbols = Describing local topological orbit structures (streamlines)

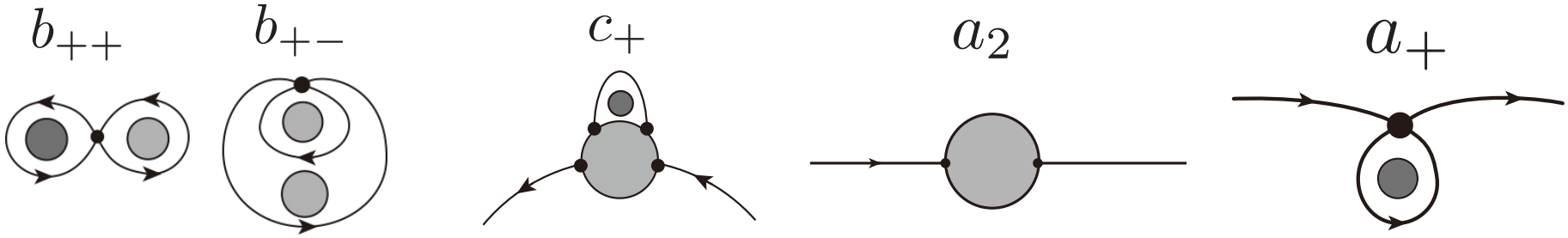

COT (= tree) & COT representation (= symbolic expression)

Instantaneous Streamlines

Topological structures

COT(=graph) & COT representation (=symbols)

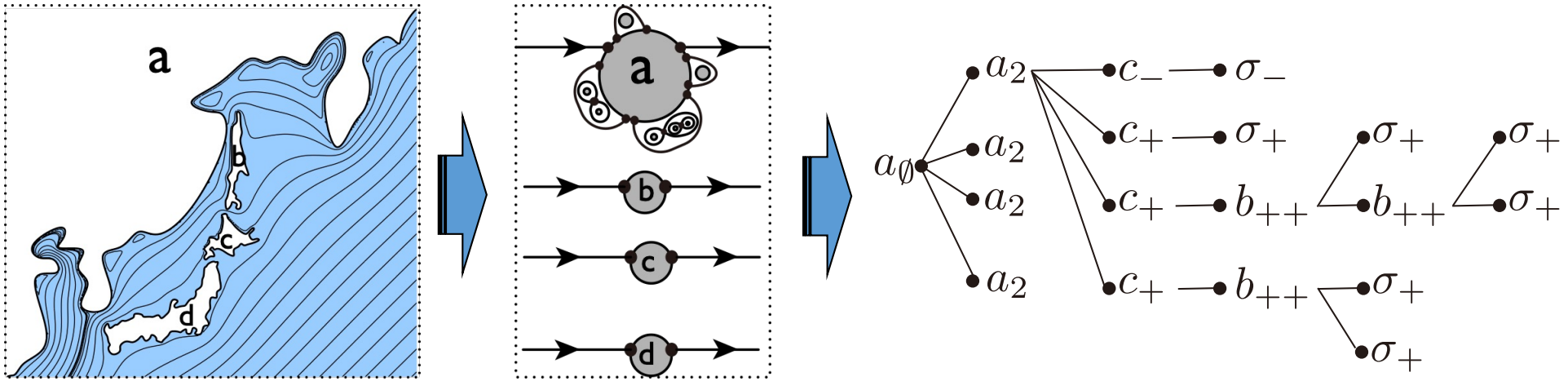

$$a_\emptyset(a_2, a_2, a_2, a_2(c_+(b_{++}\{\sigma_+, \sigma_+\}), c_+(b_{++}\{b_{++}\{\sigma_+, \sigma_+\}, \sigma_+\}), c_+(\sigma_+), c_-(\sigma_-))$$

The correspondence between the topological structures of orbits and the COT is one-to-one.

Topological Decomposition of Flow Domain

Each COT symbol is associated with a bounded region = **The region of influence**

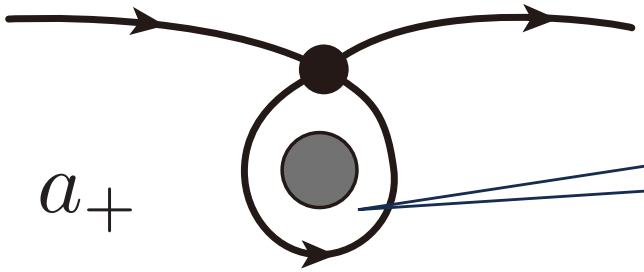

The region of influence of a_+= a flow domain enclosed by saddle separatrix

Using COT representation, the flow domain is decomposed into the regions of influence

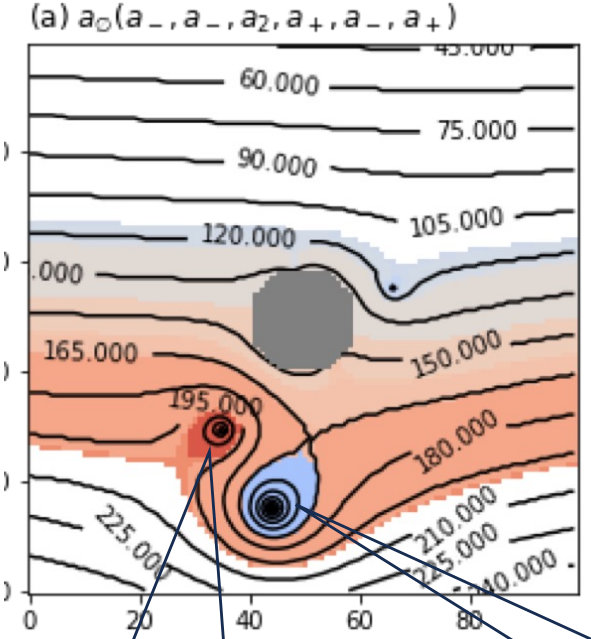

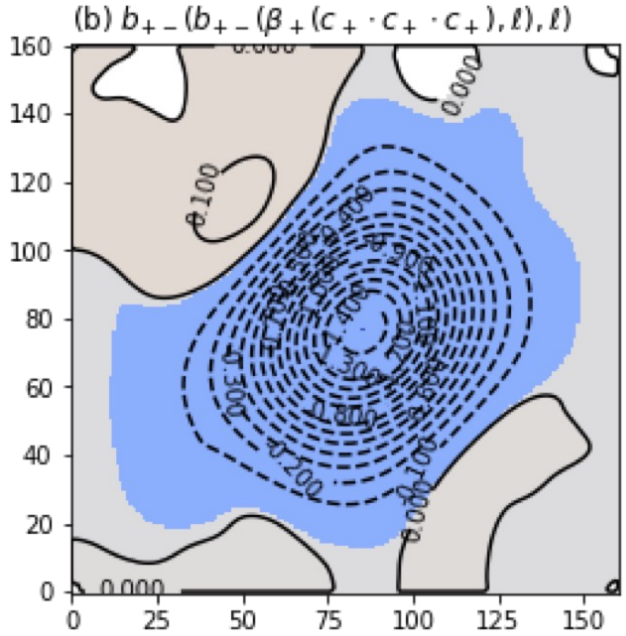

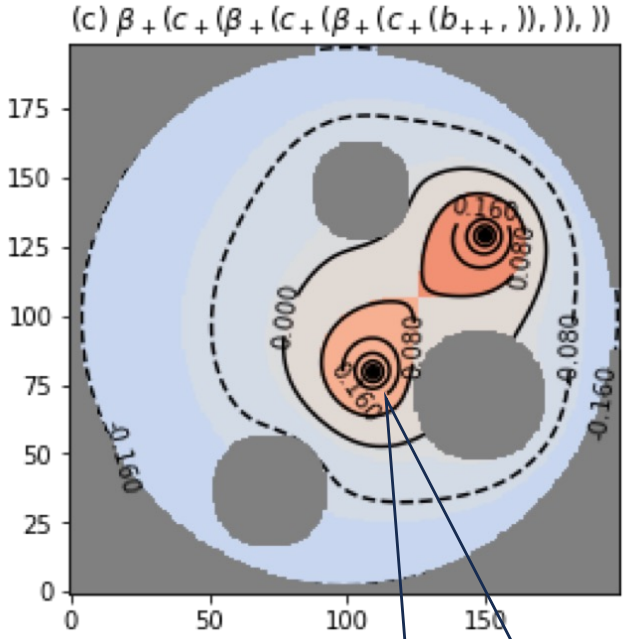

The region of influence of a_+

The region of influence of a_-

The region of influence of b_{++}

Application 1: Atmospheric Flows

Geopotential height at 500hPa (Data from Japan's Meteorological Agency)

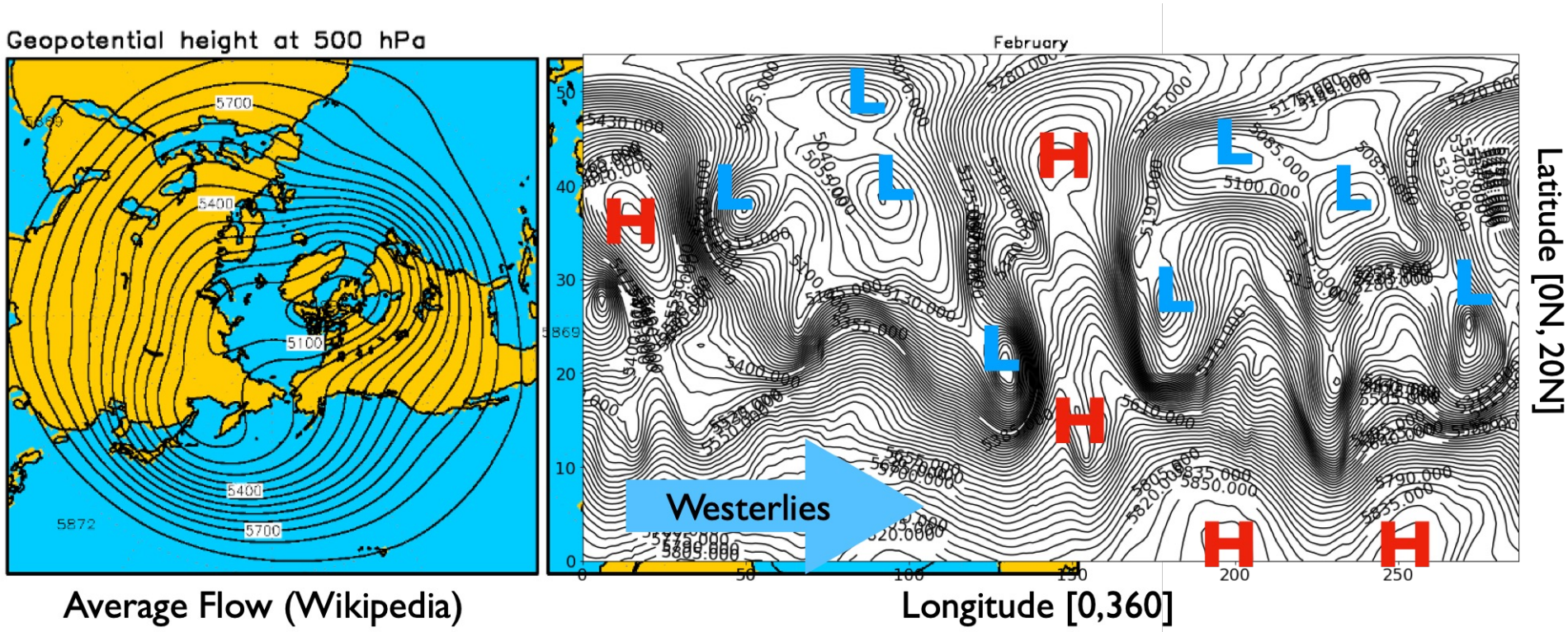

- ✓ The height of the atmosphere where the pressure becomes 500hPa.
- ✓ Under the quasi-geostrophic assumption, level curves of the geo-potential height are equivalent to streamline, yielding Hamiltonian vector fields
- ✓ Existence of westerly jet flow around the north pole.
- ✓ High/low-pressure regions play a significant role in weather/climate.

Blocking phenomena

Atmospheric Blocks (by Wikipedia):

A large-scale pattern in the atmospheric pressure field that is nearly stationary, effectively "blocking" or redirecting migratory cyclones. These blocks can remain in place for several days or even weeks, causing the areas affected by them to have the same kind of weather for an extended period of time – a cause of abnormal weather heatwaves, draught, heavy rain etc…

A "block" over western North America in 2006 (Wikipedia)

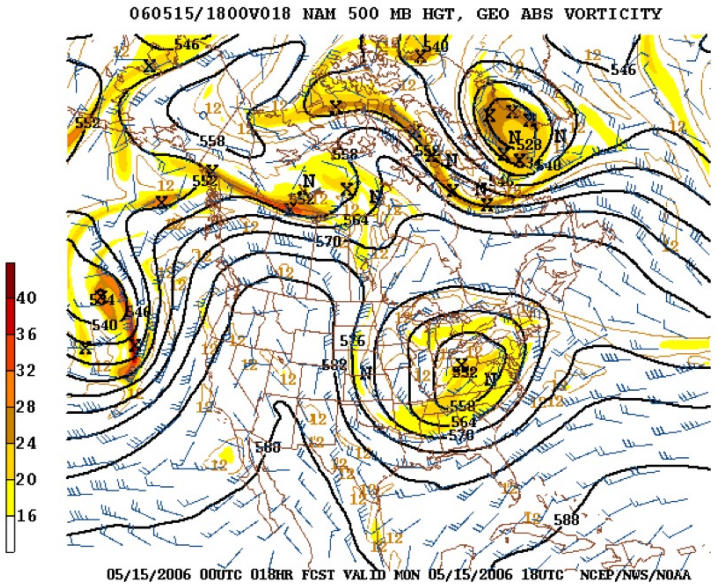

- ✓ It is difficult to identify whether or not the current weather is in the state of blocks.
- ✓ They are usually identified by experts in meteorology authority.
- ✓ We need an objective method to identify the blocking state.

Blocking morphology and COT symbols

Dipole type

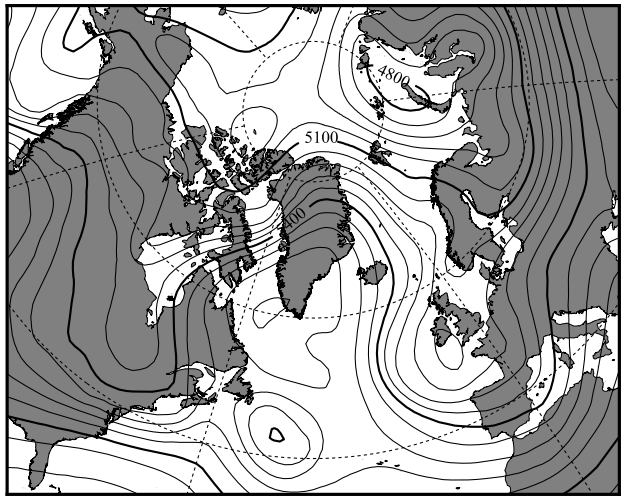

Local Morphology

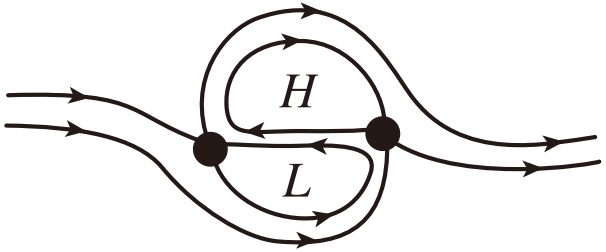

COT $a_+ \cdot a_-$

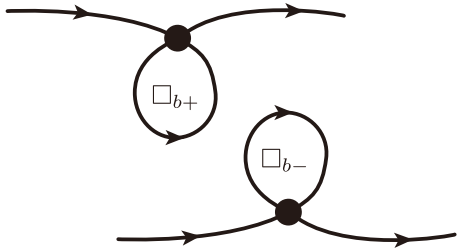

Dipole type blocking = a pair of high and low-pressure regions, which is represented by a sequence of COT symbols "$a_+ \cdot a_-$"

Ω type

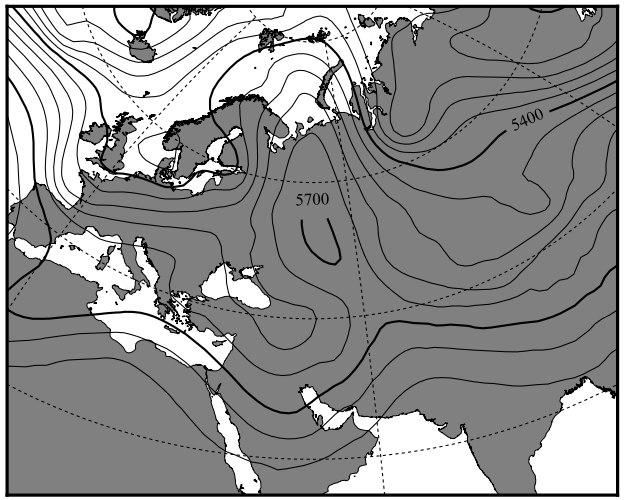

Local Morphology

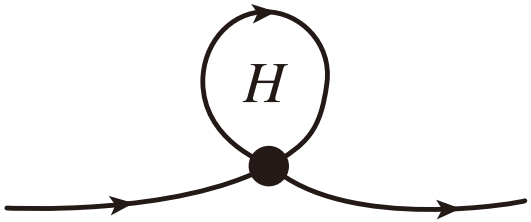

COT a_+

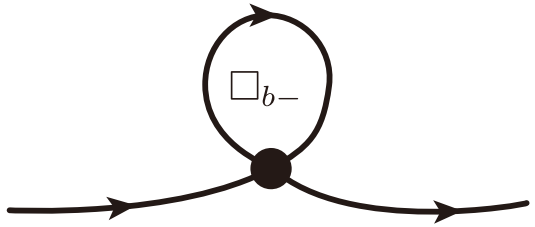

Omega type blocking = an isolated high pressure region, which is represented by a sequence of COT symbols "a_+"

Extracting information from data

With TFDA, we track the regions of influence associated with a_+ (high-pressure) and a_- (low pressures) that stay at the same locations for a longer period.

Step 1: If x is contained in the regions of influence in the time period window $s \in [t-\Delta t/2, t+\Delta t/2]$, we add the value $1s$ at $x \rightarrow \Delta t=16$ （A histogram for 48 hours is created.)

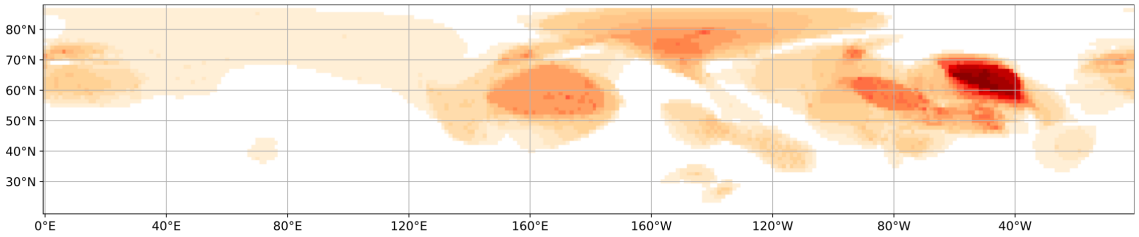

Step 2: Cutting off the histogram below $h=8$, we obtain a set of connected components.

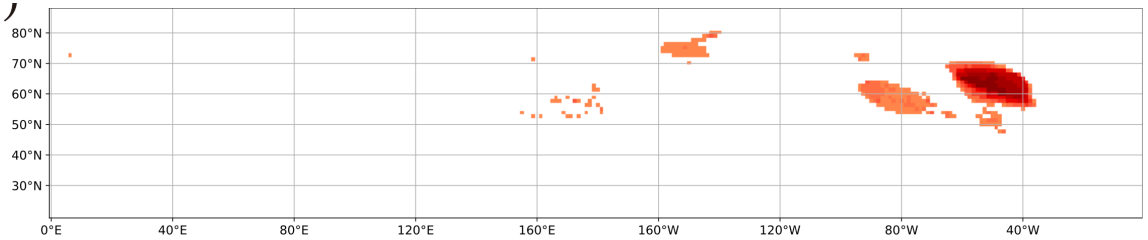

Step 3: If the geometric center of a connected component at time t is contained in a connected component at time $t-1$, a link is created between them. We then obtain a directed graph between linked components in the candidate set.

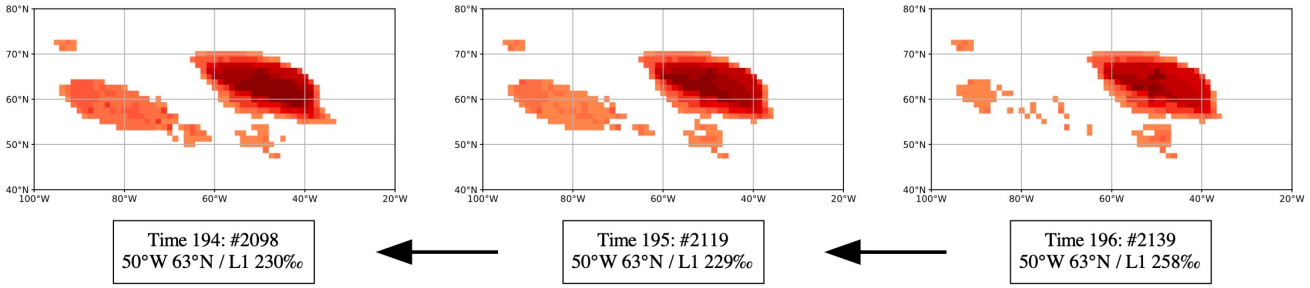

TFDA algorithm (detection of blocking)

Step 4: We remove the node of the graph whose the relative L1 norm of the difference between the histogram and the uniform distribution with Δt =16 is smaller than 0.3.

The link of nodes whose length is larger than two (12 hours) is regarded as the period of "a blocking event".

Step 5: We check the COT representation of the connected component in the intermediate node.

If the connected component is the region of influence of a_+ only, the blocking event is of Ω-type. If it is the region of influence of a pair of $a_+ \cdot a_-$, it is a dipole-type blocking.

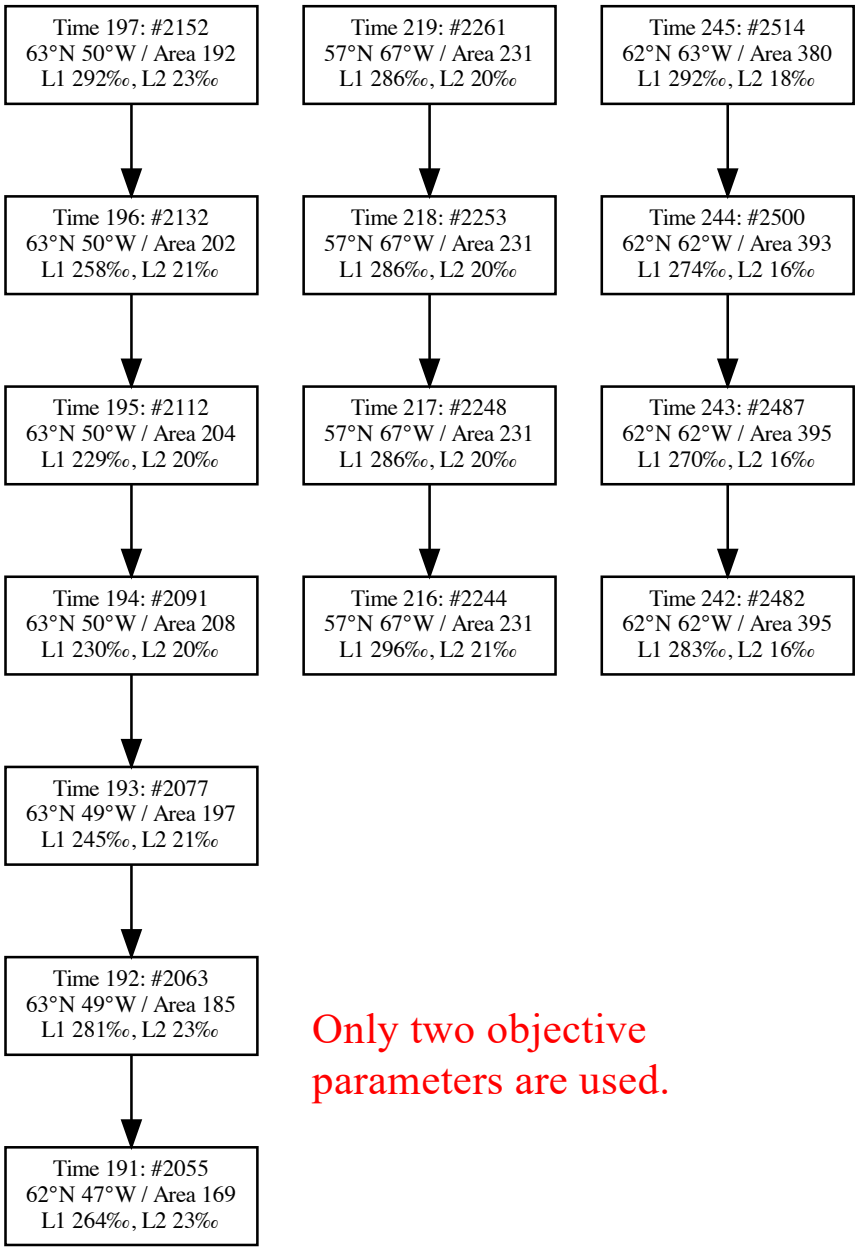

Only two objective parameters are used.

Comparison with a standard method

■ Algorithm by Dunn-Sigouin et al. (2013)

- Checking the deviation from the 6-hours average of the geo-potential height at 500hPa.
- Extracting the domains over 30 degrees North latitude whose deviation is larger than 117m (in July) and 188m (in January)
- Domains satisfying the following three conditions are regarded as the blocking regions.
  1. Area is larger than $2.5 \times 10^6 km^2$
  2. 84% of the two sequential domains are overlapped.
  3. The domain persist over 96 hours.

■ Many meteorological parameters are contained.

	TFDA ○	TFDA ×	Total
Dunn-Sigouin ○	14	7	21
Dunn-Sigouin ×	11	—	11
Total	25	7	32

A new feature: morphology identification

(a) blocking event #01 (Omega type)

$$a_{\varnothing}(a_{-}(b_{-+}(b_{--}\{\sigma_{-}, b_{--}\{\sigma_{-}, b_{--}\}\}, \sigma_{+})) \cdot a_{-}(b_{--}) \cdot a_{-} \cdot a_{-}(b_{--}) \cdot a_{-} \cdot a_{+} \cdot a_{+} \cdot a_{-} \cdot a_{+})$$

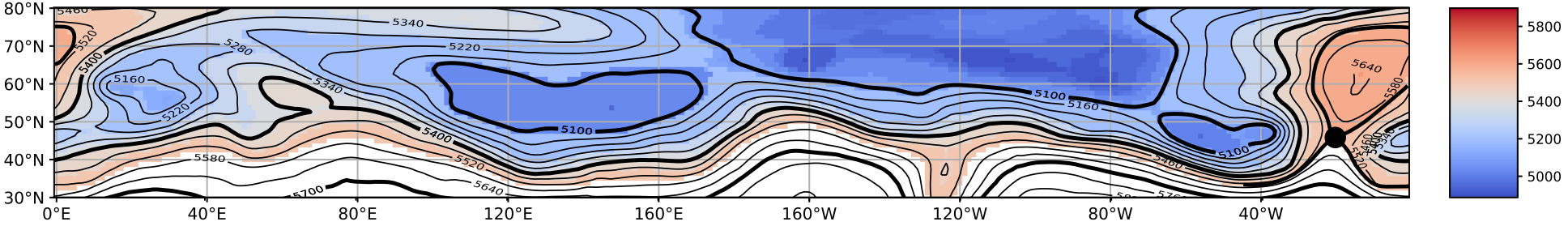

(b) blocking event #03 (Dipole type)

$$a_{\varnothing}(a_{-}(b_{--}) \cdot a_{-} \cdot a_{-} \cdot a_{-}(b_{--}) \cdot a_{-} \cdot a_{-} \cdot a_{+} \cdot a_{-} \cdot a_{-} \cdot a_{+}(b_{+-}) \cdot a_{-} \cdot a_{-})$$

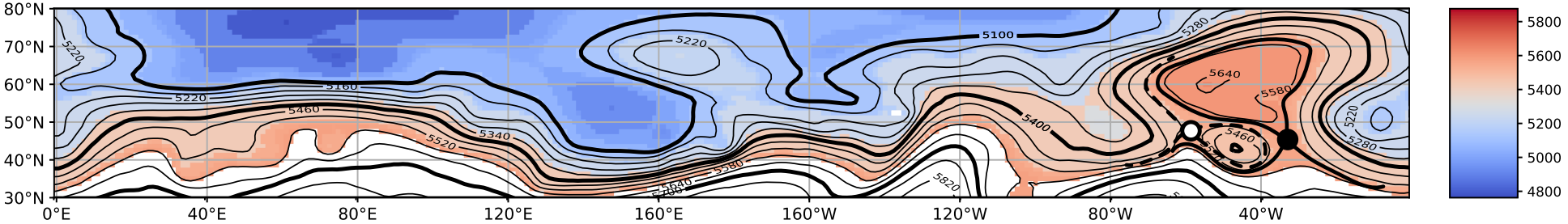

- While both algorithm detect the blocking event, TFDA can identify the morphological type of the blocking by observing the COT representation.
- A useful information in the field of atmospheric science (meteorology).

Application 2: Detection of Kuroshio Large Meandering

■ Three typical paths in Kuroshio (Kawabe'95)

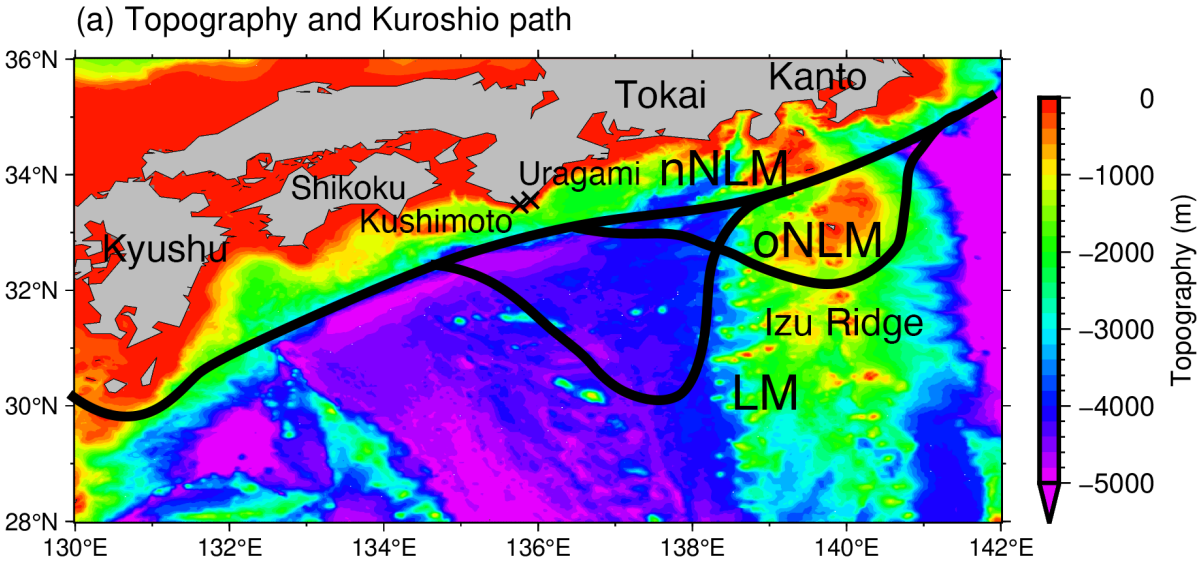

- nNLM (nearshore NonLarge Meander)
- oNLM (offshore NonLarge Meander)
- LM (Large Meander)

■ Impacts

- Ocean (Marine transport, Fishery)
- Atmosphere (Heavy snow & Hot summer in Kanto area, Nakamura et al. 2012, Sugimoto et al. 2020)

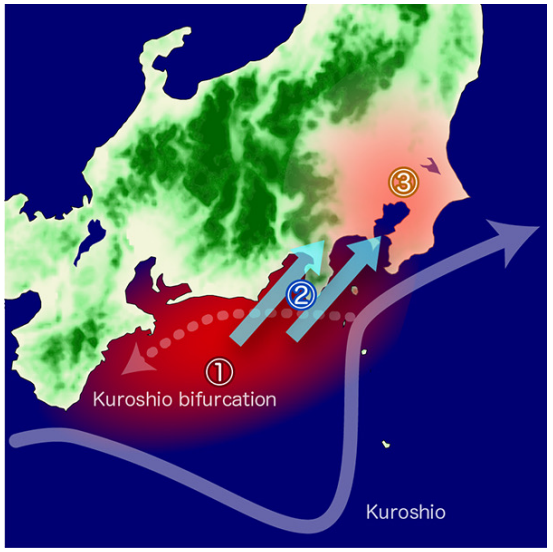

Identification of Kuroshio LM by JMA

- Japan Meteorological Agency (JMA)
  - Kuroshio's southernmost position from the temperature at sea surface and 100 m depth

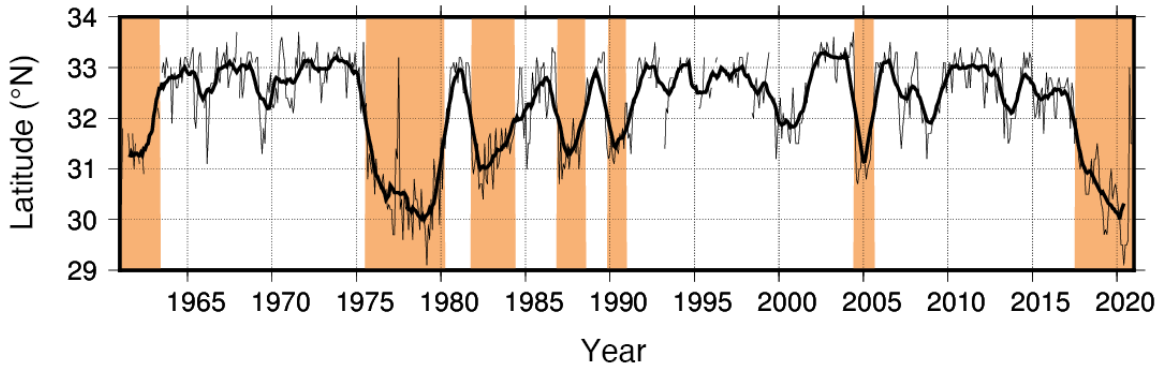

  - Sea level differences between Kushimoto and Uragami (Kawabe 1980)

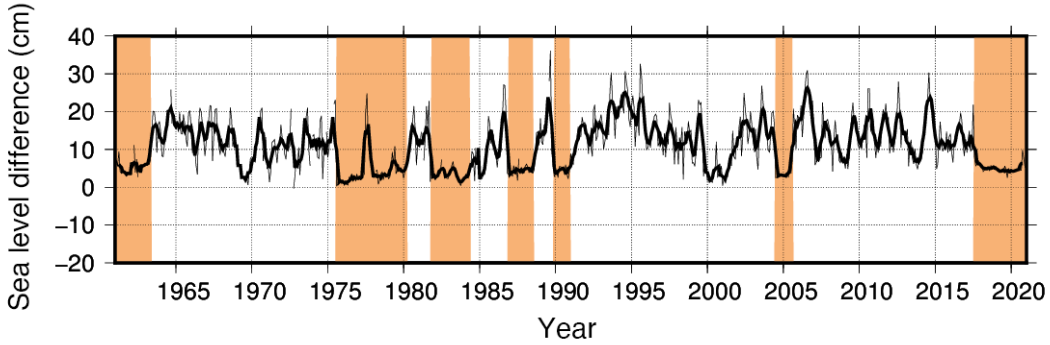

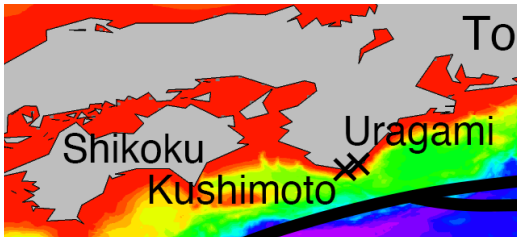

→ An empirical combination of the indicators to detect LM (orange)

- Complicated flow field with abundant fronts and eddies

→ An objective algorithm is necessary.

Data＝Sea Surface Height (SSH)

- Sea surface height h(x,y) : Hamiltonian of the ocean current (velocity field) under the quasi-geostrophic balance.

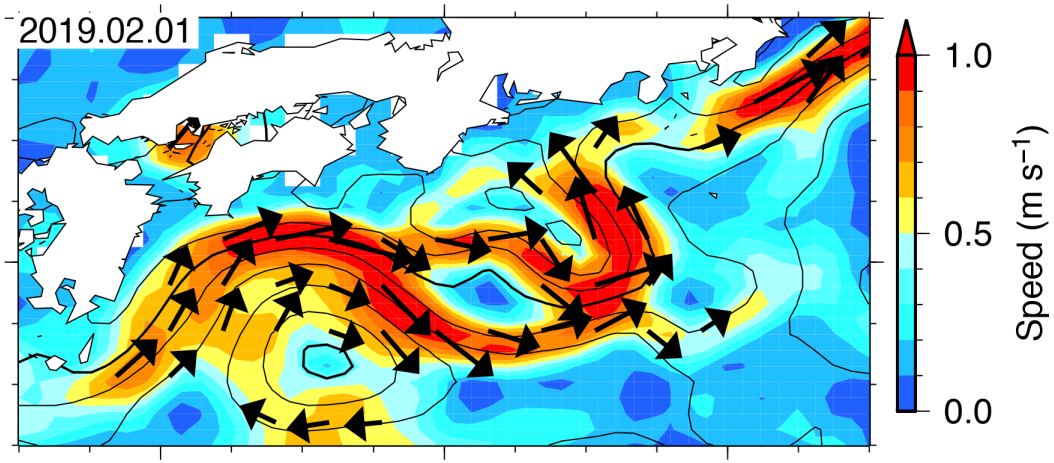

$$u_g = -\frac{g}{f}\frac{\partial h}{\partial y},\ v_g = \frac{g}{f}\frac{\partial h}{\partial x}$$

- Dataset: AVISO (Ducet et al. 2000)

Domain: Global → South of Japan [125–155° E, 25–45° N]
Variable: Sea surface height
Horizontal resolution: 0.25°
Temporal resolution: 1 month
Period: 1993.01–2020.05 (27 years)

Algorithm

$$a_{\emptyset}(a_{-}^{0} \cdot a_{+}^{1} \cdot a_{+}^{2} \; a_{-}^{3} \; a_{-}^{4} \cdot a_{2}(c_{+}^{0}, \lambda) \cdot a_{-}^{6} \cdot a_{-}^{7} \cdot a_{-}^{8} \cdot a_{+}^{9} \cdot a_{+}^{10}(b_{++}) \cdot a_{+}^{11})$$

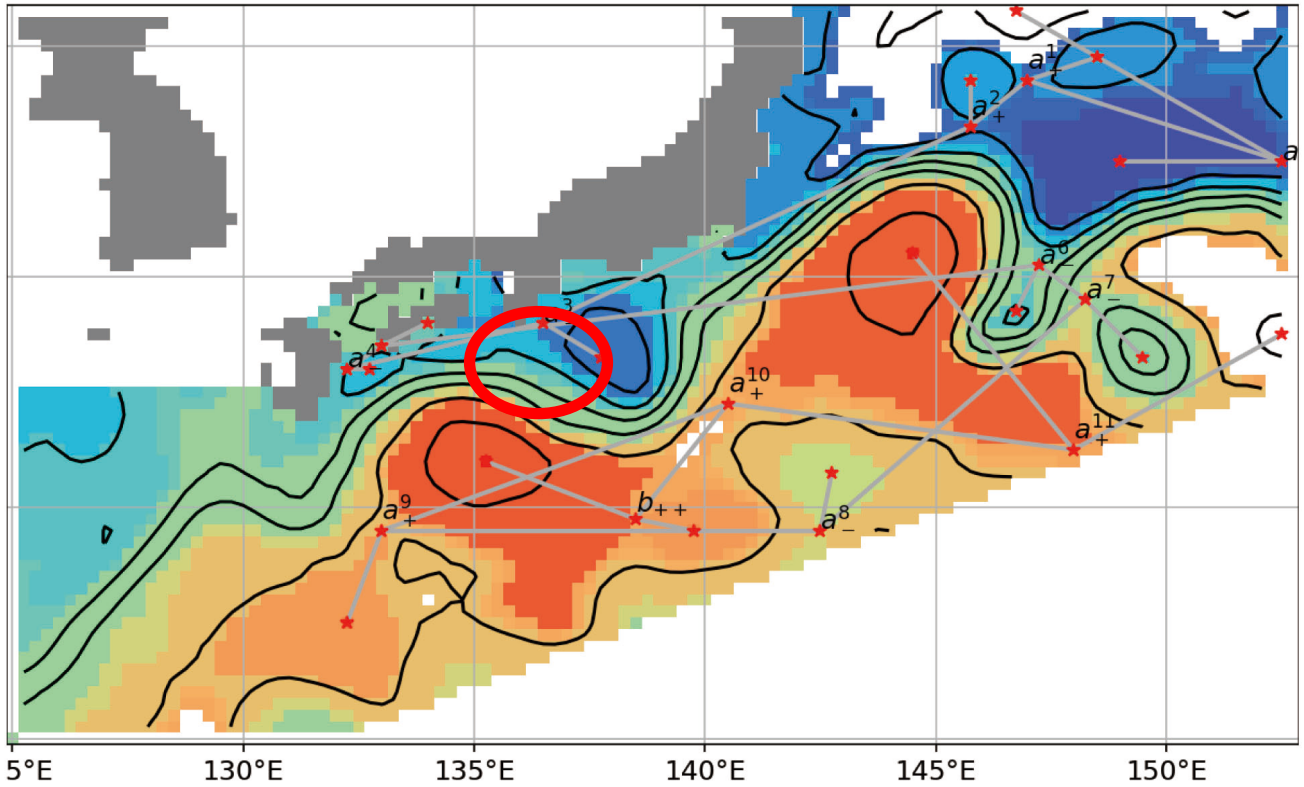

- Algorithm (the same as the blocking detection)
  - Extract the region of influence associated with a_ in the COT representations
  - Create a histogram and the domains that persist for 6 months
  - Create a chronological link between domains

Result: comparison with JMA results

- Kuroshio southernmost position off the Tokai district (136° –140° E)
  TFDA: Southernmost latitude of cyclonic eddies

- Meandering events detected by TFDA
  - Episode A: 2004.09–2005.06 (JMA: 2004.07–2005.08)
  - Episode B: 2013.10–2014.02
  - Episode C: 2016.09–2016.12
  - Episode D & E: 2017.10–2019.03, 2019.09– (JMA: 2017.08–)
    - ⇨ A, D, E are detected by JMA and TFDA, while B and C are not detected by JMA.

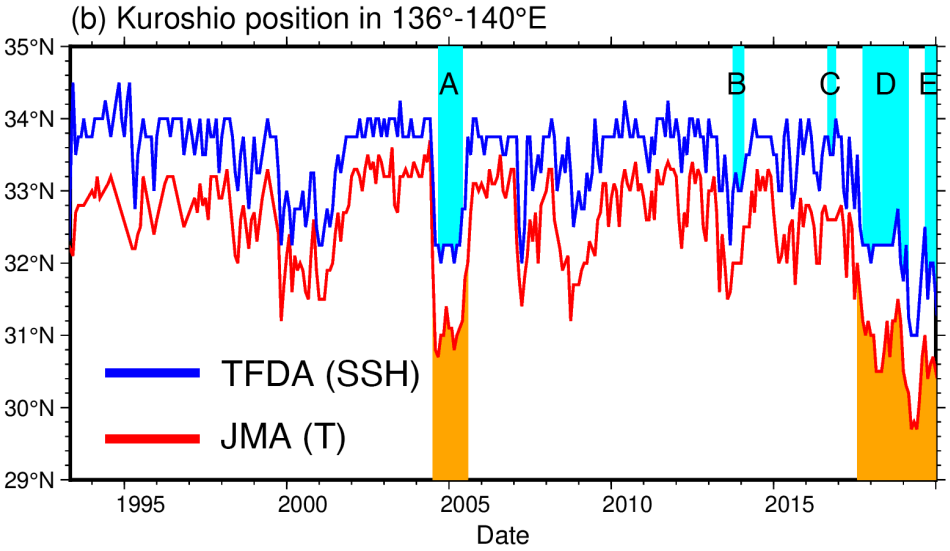

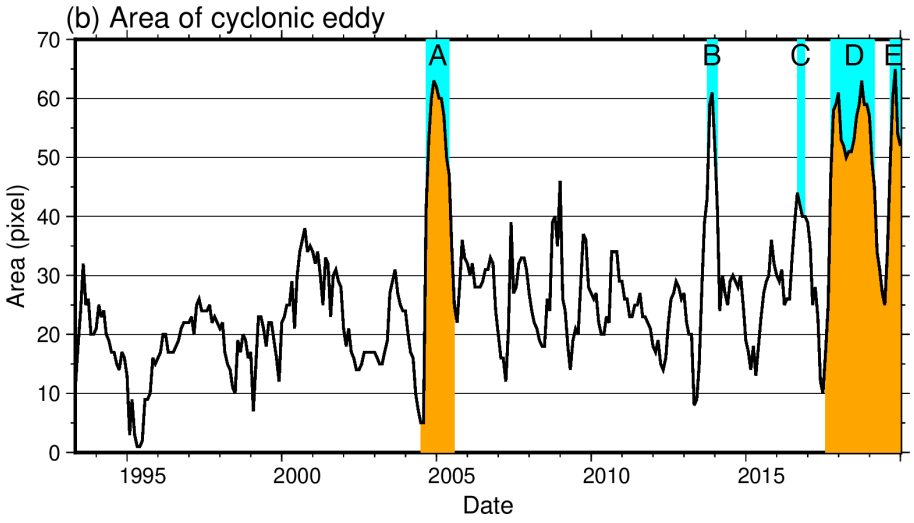

Result: classification of types

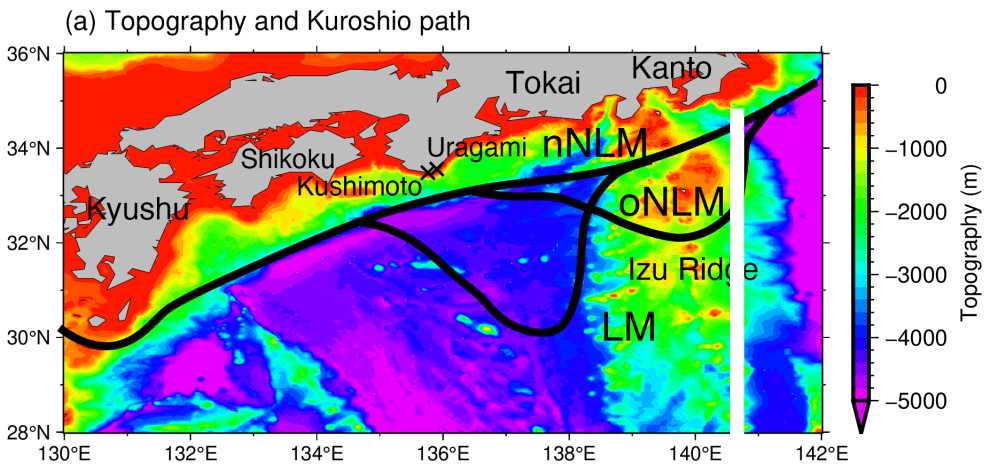

Along 140° E, the Kuroshio is located

- near the coast during the LM
- off the coast during the oNLM

Episode A (TFDA and JMA)

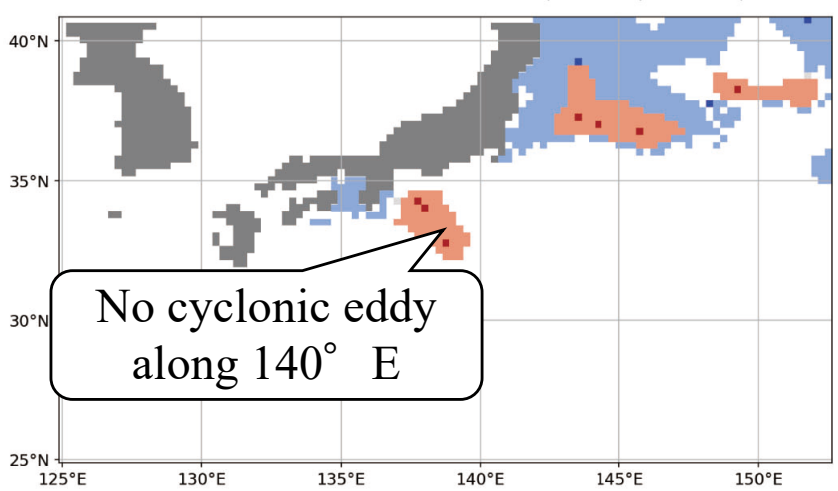

Episode B (TFDA)

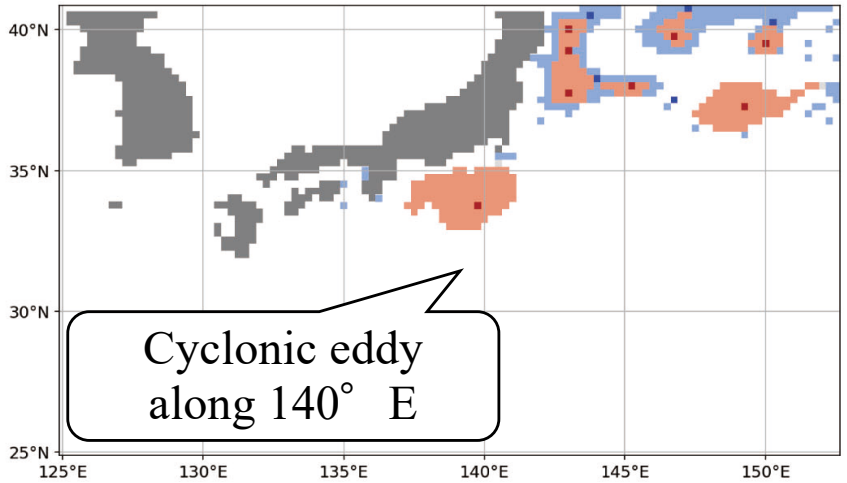

⇨ A, D, E are LM, but B and C are oNLM !

⇨ TFDA can detect oNLM, but JMA cannot.

Result: Symptom of the termination of KLM

- Figure-eight-shaped eddy b_ _ is detected when meandering events are terminated

Eight-shaped eddies

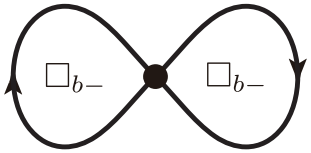

$b_{--}\{\square_{b_-}, \square_{b_-}\}$

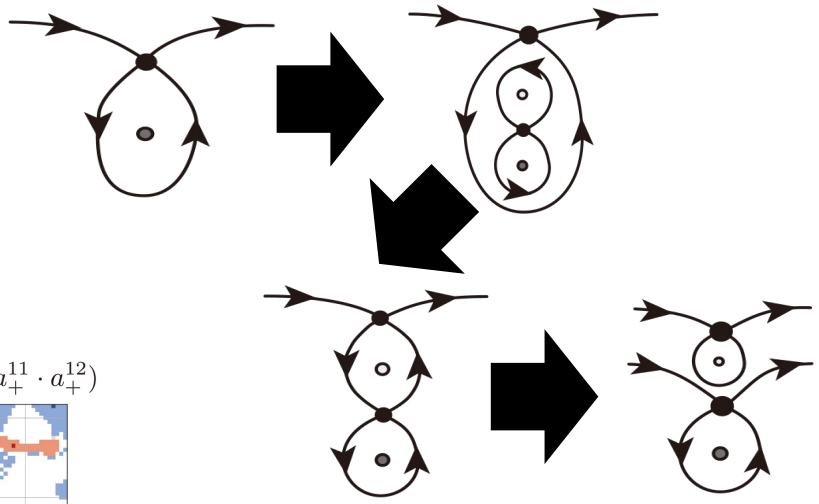

(a) t=200505 $a_\emptyset(a^0_-(b_{--}) \cdot a^1_- \cdot a^2_+ \cdot a^3_+ \cdot a^4_-(b_{--}) \cdot a_2 \cdot a^6_- \cdot a^7_- \cdot a^8_- \cdot a^9_+ \cdot a^{10}_+ \cdot a^{11}_+ \cdot a^{12}_+)$

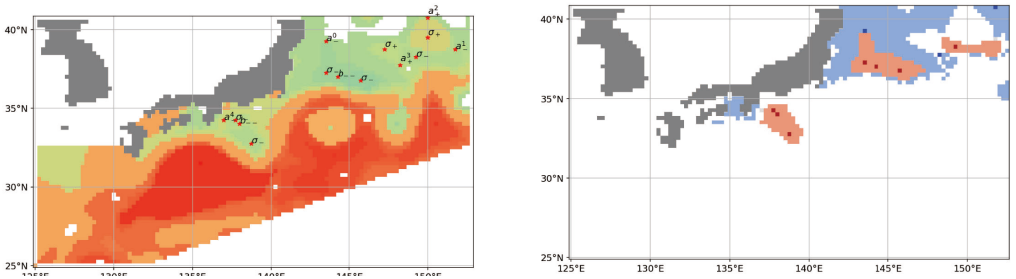

(b) t=201904 $a_\emptyset(a^0_- \cdot a^1_+ \cdot a^2_+ \cdot a^3_-(b_{--}) \cdot a^4_- \cdot a^5_+ \cdot a_2(c^0_+, \lambda_-) \cdot a^7_- \cdot a^8_+ \cdot a^9_- \cdot a^{10}_- \cdot a^{11}_- \cdot a^{12}_- \cdot a^{13}_+ \cdot a^{14}_- \cdot a^{15}_+ \cdot a^{16}_+ \cdot a^{17}_+ \cdot a^{18}_+ \cdot a^{19}_+ \cdot a^{20}_+ \cdot a^{21}_+)$

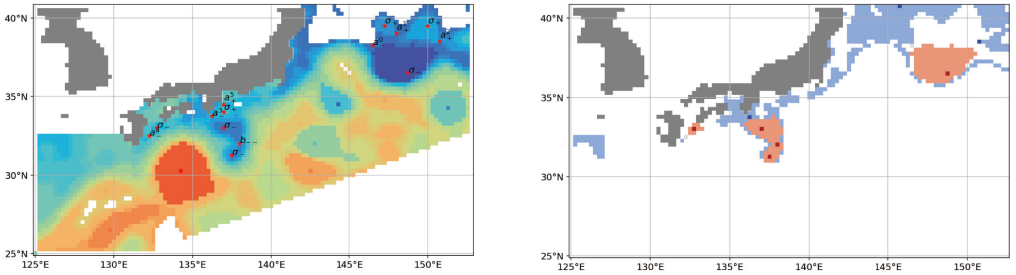

Kuroshio transport across 137°E

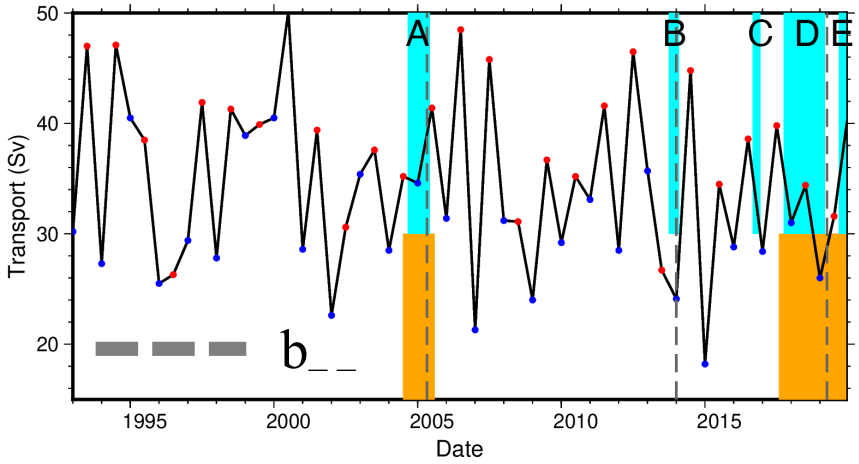

- 3 out of 4 events show b_ _ when meandering events are terminated
- This might be related to the enhancement of the Kuroshio transport

A reduced order graph model for complex flow evolutions

Example: the lid-driven cavity flow

Re=14000

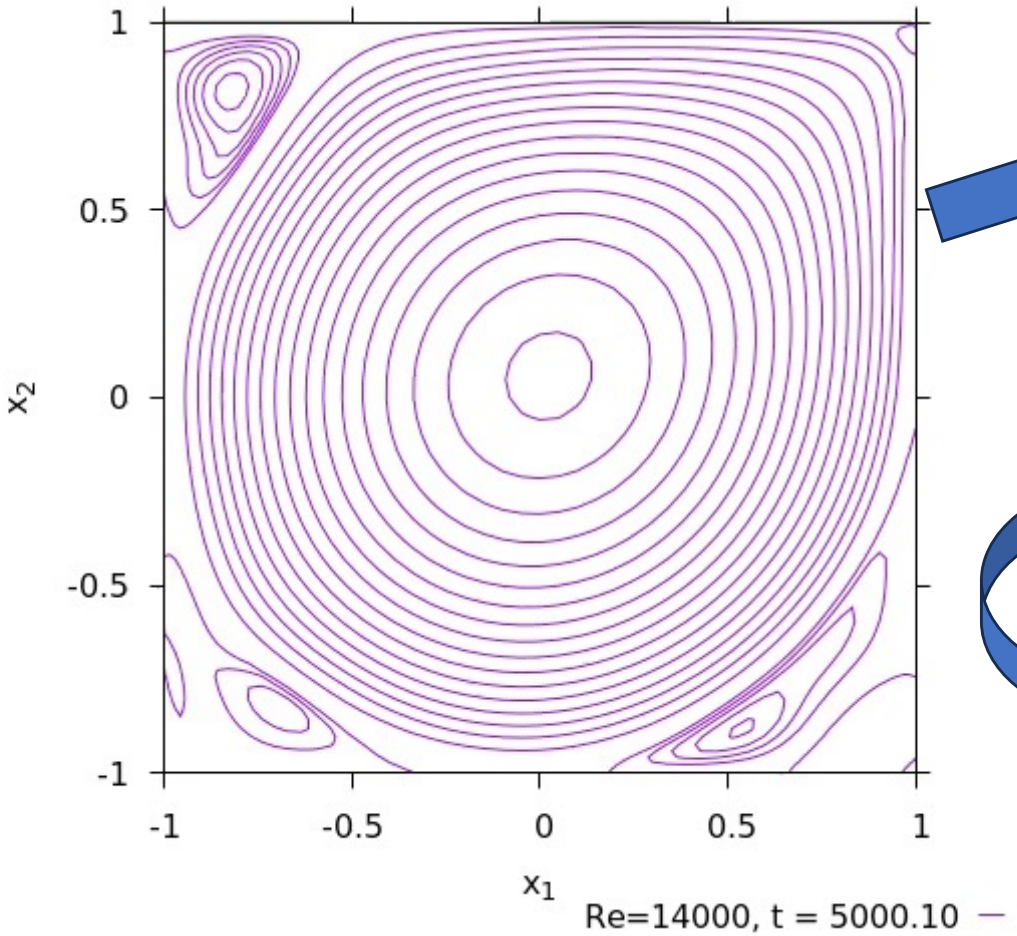

	time	time	duration	reduced_cot	loc_cot
1	5000.01	5002.77	277	c+0.c+1.c+2	B+{c+0.c+1.c+2}
2	5002.78	5003.17	40	c+0.c+0.c+1.c+2	B+{c+0.c+0.c+1.c+2}
4	5003.19	5003.96	78	c+0(b++,c-).c+1.c+1.c+2	B+{c+0(b++,L-).c+1.c+1.c+2}
5	5003.97	5004.22	26	c+0.c+1.c+1.c+2	B+{c+0.c+1.c+1.c+2}
6	5004.31	5005.03	73	c+0.c+1(b++,c-).c+2	B+{c+0.c+1(b++,L-).c+2}
7	5005.04	5007.91	288	c+0.c+1.c+2	B+{c+0.c+1.c+2}
8	5007.92	5008.31	40	c+0.c+0.c+1.c+2	B+{c+0.c+0.c+1.c+2}
10	5008.33	5009.1	78	c+0(b++,c-).c+1.c+1.c+2	B+{c+0(b++,L-).c+1.c+1.c+2}
11	5009.11	5009.36	26	c+0.c+1.c+1.c+2	B+{c+0.c+1.c+1.c+2}
12	5009.45	5010.17	73	c+0.c+1(b++,c-).c+2	B+{c+0.c+1(b++,L-).c+2}
13	5010.18	5013.05	288	c+0.c+1.c+2	B+{c+0.c+1.c+2}
14	5013.06	5013.45	40	c+0.c+0.c+1.c+2	B+{c+0.c+0.c+1.c+2}
16	5013.47	5014.24	78	c+0(b++,c-).c+1.c+1.c+2	B+{c+0(b++,L-).c+1.c+1.c+2}
17	5014.25	5014.5	26	c+0.c+1.c+1.c+2	B+{c+0.c+1.c+1.c+2}
18	5014.59	5015.31	73	c+0.c+1(b++,c-).c+2	B+{c+0.c+1(b++,L-).c+2}
19	5015.32	5018.19	288	c+0.c+1.c+2	B+{c+0.c+1.c+2}
20	5018.2	5018.59	40	c+0.c+0.c+1.c+2	B+{c+0.c+0.c+1.c+2}
22	5018.61	5019.38	78	c+0(b++,c-).c+1.c+1.c+2	B+{c+0(b++,L-).c+1.c+1.c+2}
23	5019.39	5019.64	26	c+0.c+1.c+1.c+2	B+{c+0.c+1.c+1.c+2}
24	5019.73	5020.45	73	c+0.c+1(b++,c-).c+2	B+{c+0.c+1(b++,L-).c+2}
25	5020.46	5023.33	288	c+0.c+1.c+2	B+{c+0.c+1.c+2}

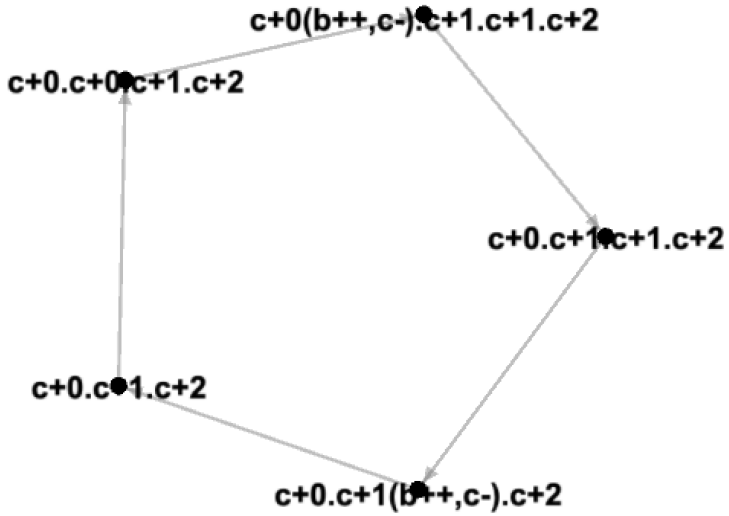

The evolution of flow patterns are converted into a transition graph between COTs

Graph Analysis

Re=14000

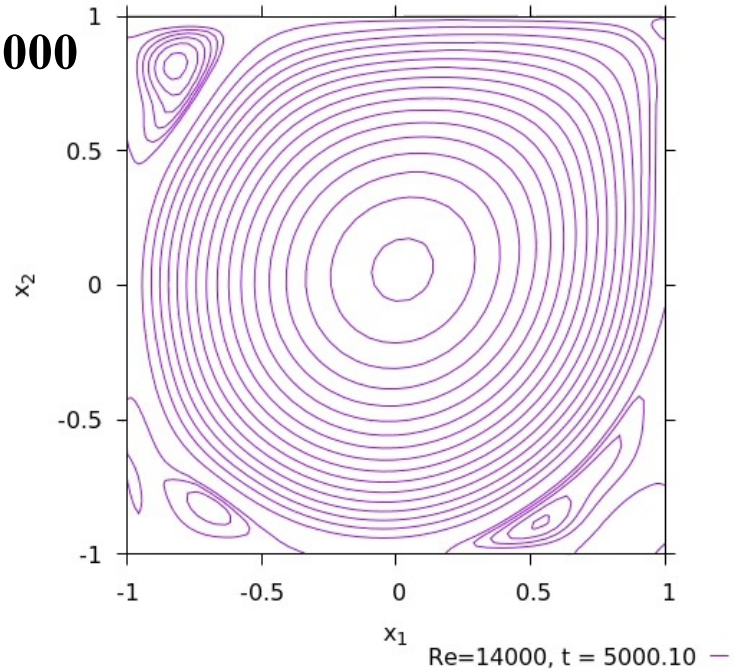

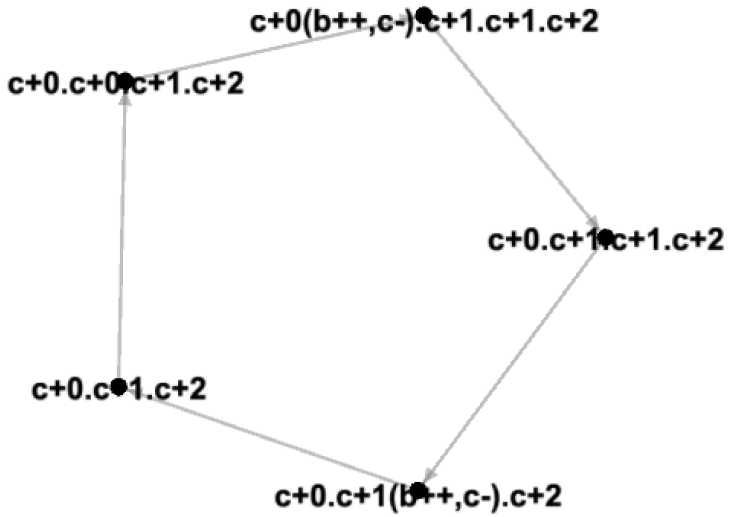

Re=16000

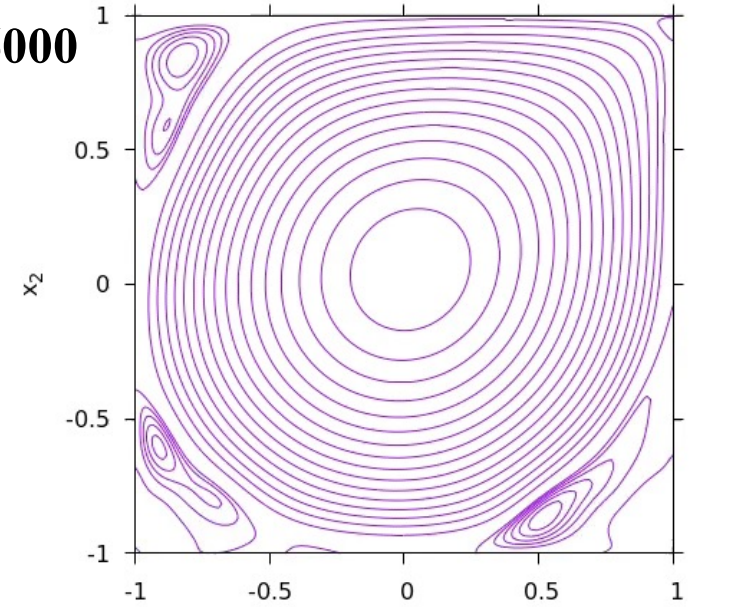

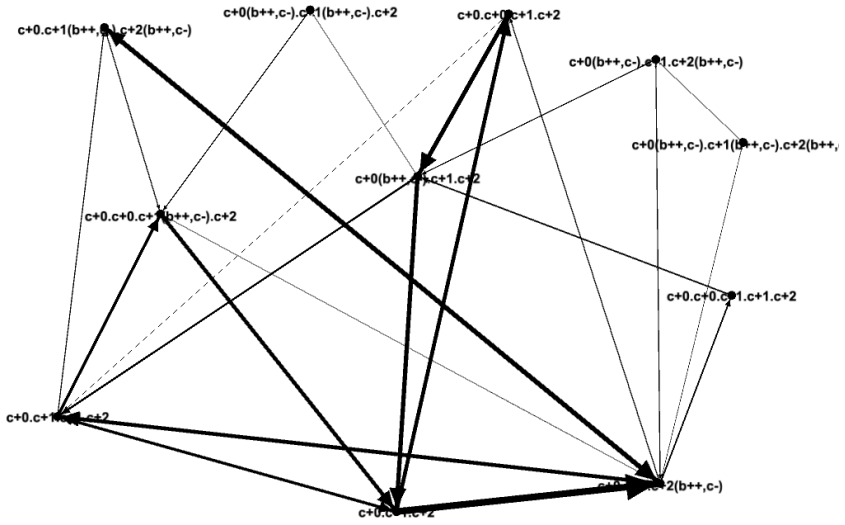

The evolution of flow patterns are converted into a transition graph between COTs